# Quantifying the Donor–Acceptor Properties of Carbon Monoxide and Its Carbo-mer Using ELF Analysis

**ARTICLE** *in* ORGANOMETALLICS · SEPTEMBER 2008

Impact Factor: 4.13 · DOI: 10.1021/om800578c



**4 AUTHORS**, INCLUDING:

Jean-Marie Ducéré
University of Toulouse
**29** PUBLICATIONS **284** CITATIONS
SEE PROFILE

Remi Chauvin
Laboratoire de Chimie de Coordination.
**167** PUBLICATIONS **1,952** CITATIONS
SEE PROFILE

# Quantifying the Donor−Acceptor Properties of Carbon Monoxide and Its *Carbo*-mer Using ELF Analysis

Jean-Marie Ducéré,[§] Christine Lepetit,*[,†] Bernard Silvi,*[,‡] and Remi Chauvin*[,†]

*Laboratoire de Chimie de Coordination, UPR 8241 CNRS, 205 Route de Narbonne, 31 077 Toulouse Cedex 4, France, Laboratoire de Chimie Théorique, UMR 7616 CNRS, Université Pierre et Marie Curie, Site le Raphaël, 3 rue Galilée, 94200 Ivry sur Seine, France, and LAAS-CNRS, Université de Toulouse, 7 avenue du Colonel Roche, F-31077 Toulouse, France*

*Received June 23, 2008*

The coordinating properties to nickel of CO and its *carbo*-mer $C_3O$ are compared on the basis of computational studies of $Ni(CO)_4$ and $Ni(C_3O)(CO)_3$. The Ni−$C_3O$ bond is predicted to be stronger than the corresponding Ni−CO bond. Electron localization function (ELF) and atoms-in-molecules (AIM) analyses are used to estimate the donation and back-donation contributions to the net charge transfer involved in the corresponding nickel complexes of CO and $C_3O$. The $\sigma$-donating and $\pi$-accepting properties for $C_3O$ toward $Ni(CO)_3$ are slightly stronger than for its CO parent. In both cases, however, $\pi$-back-donation is the major electron transfer process.

## Introduction

Since its matrix isolation (and determination of its IR band at 2244 $cm^{-1}$) in 1971[1] and its synthesis in the gas phase in 1983,[2] tricarbon monoxide ($C_3O$) has been extensively studied in argon matrices[3] and for its involvment in the chemistry of interstellar and circumstellar gas clouds.[4]

The heterocumulene $C_3O$ may also be considered as the *carbo*-mer of carbon monoxide,[5] and consequently, it is the first member of the recently investigated family of *carbo*-[*n*]oxocarbons.[6] However, in contrast to its parent, the coordination chemistry of *carbo*-CO remains to be explored. On the basis of IR and $^{13}C$ NMR spectroscopy, $C_3O$ was indeed reported to be a stable ligand of chromium pentacarbonyl (Scheme 1: $n = 6$, L = CO).[7a] To the best of our knowledge, this is the only report on transition-metal coordination of $C_3O$. It can also be mentioned that the isostructural complex $Cr(CO)_5(CNCN)$ of the isocyanogen ligand CNCN has also been studied.[7b] In the spirit of the *carbo*-meric comparison, the influence of *carbo*-merization on the coordinating properties of CO is hereafter addressed (Scheme 1). The possibility and strength of coordination to nickel will be examined from computational studies, and the donor−acceptor properties of *carbo*-CO will be compared to those of its parent within the Dewar−Chatt−Duncanson (DCD) model.[8]

**Scheme 1. Synoptic View of the Two Comparative Studies of the CO Ligand versus Its *Carbo*-mer**

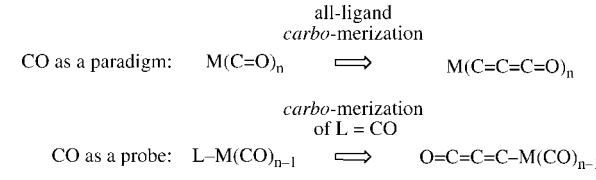


According to the DCD analysis, coordination of carbon monoxide to transition metals involves two synergistic interactions contributing to the metal−CO bonds. The $\sigma$ HOMO of CO donates electron density to the empty dsp-hybrid ($\sigma$) LUMO of the transition-metal fragment ($\sigma$-donation). The metal simultaneously donates electron density from its d($\pi$) HOMOs into the empty $\pi^*$ LUMO of CO ($\pi$-back-donation). This "adaptative two-way communication" makes the CO ligand a versatile probe for the electronic properties of other co-ligands, such as phosphanes (Tolman's electronic parameter with respect to the $Ni(CO)_3$ fragment),[9] N-heterocyclic carbenes, and ylides (with respect to the $Ni(CO)_3$ or the $Rh(CO)_2$ fragment).[10] Variations of the CO ligand properties (IR stretching frequencies, $^{13}C$ NMR chemical shifts) thus serve to quantify the overall donor−acceptor properties of the studied co-ligand. Theoretical methods are however often required for the separation of donation and back-donation effects. Indeed, computational methods proved to be reliable for reproducing/predicting the experimental observables,

* Corresponding authors. E-mail: christine.lepetit@lcc-toulouse.fr; silvi@lct.jussieu.fr; remi.chauvin@lcc-toulouse.fr.
† Laboratoire de Chimie de Coordination, UPR 8241 CNRS.
‡ Laboratoire de Chimie Théorique, UMR 7616 CNRS.
§ LAAS-CNRS, Université de Toulouse.

(1) DeKock, R. L.; Weltner, W. *J. Am. Chem. Soc.* **1971**, *93*, 7106.
(2) Brown, R. D.; Eastwood, F. W.; Elmes, P. S.; Godfrey, P. D. *J. Am. Chem. Soc.* **1983**, *105*, 6496.
(3) (a) Brown, R. D.; Godfrey, P. D.; Elmes, P. S.; Rodler, M.; Tack, L. M. *J. Am. Chem. Soc.* **1985**, *107*, 4112. (b) Brown, R. D.; Pullin, D. E.; Rice, E. H. N.; Rodler, M. *J. Am. Chem. Soc.* **1985**, *107*, 7877.
(4) (a) Tenenbaum, E. D.; Apponi, A. J.; Ziurys, L. M.; Agundez, M.; Cernicharo, J.; Pardo, J. R.; Guelin, M. *Astrophys. J. Lett.* **2006**, *649*, L17. (b) Jamieson, C. S.; Mebel, A. M.; Kaiser, R. I. *Astrophys. J. Suppl. Ser.* **2006**, *163*, 184. (c) Woon, D. W.; Herbst, E. *Astrophys. J.* **1996**, *465*, 795. (d) Brown, R. D.; Godfrey, P. D.; Cragg, D. M.; Rice, E. H. N.; Irvine, W. M.; Friberg, P.; Suzuki, H.; Ohishi, M.; Kaifu, N.; Morimoto, M. *Astrophys. J.* **1985**, *297*, 302.
(5) (a) Chauvin, R. *Tetrahedron Lett.* **1995**, *36*, 397. (b) Maraval, V.; Chauvin, R. *Chem. Rev.* **2006**, *106*, 5317.
(6) (a) Lepetit, C.; Chermette, H.; Gicquel, M.; Heully, J.-L.; Chauvin, R. *J. Phys. Chem. A* **2007**, *111*, 136. (b) Gicquel, M.; Lepetit, C.; Heully, J.-L.; Chauvin, R. *Phys. Chem. Chem. Phys.* **2008**, *10*, 3578.
(7) (a) Berke, H.; Härter, P. *Angew. Chem., Int. Ed. Engl.* **1980**, *19*, 225. (b) Aarnts, M. P.; Stufkens, D. J.; Sola, M.; Baerends, E. J. *Organometallics* **1997**, *16*, 2254.
(8) (a) Dewar, M. J. S. *Bull. Soc. Chim. Fr* **1951**, *18*, C79. (b) Chatt, J.; Duncanson, L. A. *J. Chem. Soc.* **1953**, *2929*.
(9) Tolman, C. A. *J. Am. Chem. Soc.* **1970**, *92*, 2953.
(10) (a) Dorta, R.; Stevens, E. D.; Scott, N. M.; Costabile, C.; Cavallo, L.; Hoff, C. D.; Nolan, S. P. *J. Am. Chem. Soc.* **2005**, *127*, 2485. (b) Canac, Y.; Lepetit, C.; Abdalilah, M.; Duhayon, C.; Chauvin, R. *J. Am. Chem. Soc.* **2008**, *130*, 8406.

10.1021/om800578c CCC: $40.75 
Publication on Web 09/18/2008

but also meaningful for analyzing the orbital/electronic origin of their values. Such computational investigations were mostly based on interaction-energy partition schemes such as energy decomposition analysis (EDA)[11] or constrained space orbital variation (CSOV).[12] Schemes based on valence bond[13] or on the natural orbitals for chemical valence (NOCV)[14] were also recently reported.

The selected approach for the quantification of donor−acceptor properties of CO and its *carbo*-mer is inspired from a recently disclosed method, based on ELF and AIM partitions, that provided a relevant donation/back-donation scheme in metal monocarbonyls.[15]

## Computational Details

Geometries were fully optimized under symmetry constraint (when possible) at the DFT level of calculation (B3LYP) using the Gaussian94[16] or Gaussian03[17] code and various basis sets.[18] Vibrational analysis was performed at the same level of calculation as the geometry optimization.

Fragment analyses were performed with the ADF2007.01 code and the TZP basis set.[19]

Frontier orbital contours were drawn with the Molekel visualization package.[20]

ELF and AIM (atoms in molecules)[21] analyses were performed with the TopMoD program.[22]

## Results and Discussion

**1. Comparison of the CO and *Carbo*-CO Calculated Structures.** The linear equilibrium geometry of the singlet ground state of $C_3O$ has been previously reported at various calculation levels. The bond lengths (1.270, 1.295, 1.150 Å, for the **:**C═C, C═CO, C═O bonds, respectively) calculated at the B3LYP/6-311+G* level in this work are in good agreement with high-level CCSD(T)/cc-pVQZ calculations (1.275, 1.300, 1.153 Å)[23] and with experimental values deduced from microwave spectroscopy (1.254, 1.306, 1.150 Å).[3,24] Botschwina and Reisenauer[25] combined experimental ground-state rotational constants and theoretical vibration−rotation coupling constants in order to suggest a more accurate geometry of $C_3O$ (1.2717, 1.2965, 1.1473 Å), which is in excellent agreement with CCSD(T)/augcc-pVTZ calculations.[26] At the same level, the rather shallow bending potential of $C_3O$ was also underlined.[27] BLYP and MP2 calculations are less satisfactory, as they yield longer C−C and C−O termini, while the bond length of the central $C_2$ unit is suitable.[28]

**1.a. Dipole Moment.** The first theoretical study of $C_3O$, performed at the SCF and MP3 levels by Brown et al., yielded acceptable geometries but an underestimated dipole moment.[29]

The experimental dipole moment of $C_3O$ (2.391 D) was deduced from Stark effects on microwave absorption transitions.[2] It is unsurprisingly larger than the experimental dipole moment of CO (0.112 D deduced from Stark effect measurements,[30] 0.1098 D measured by molecular beam electric resonance spectroscopy[31]), but as in the case of CO, it was roughly reproduced by low-level calculations (1.85 D at the SCF/6-31G* level).[29] Accurate values are obtained at the B3LYP/6-311+G* level ($\mu(C_3O) = 2.210$ D, $\mu(CO) = 0.07$ D), approaching the performance of higher levels ($\mu(C_3O) = 2.535$ D at the CEPA-1 level,[27] $\mu(CO) = 0.094$ D at the QCISD level[32]).

It is however noticeable that the dipole moments of both CO and $C_3O$ are oriented in the same direction, with the centroid of the positive charges located near the oxygen end of the molecules (Figure 1): as in the case of CO, this could be a driving force for the C-complexation of $C_3O$ to transition metals.

**1.b. Frontier Orbitals.** The frontier orbitals of *carbo*-CO are compared to those of its parent CO in Figure 1. In both cases, the $\sigma$-type HOMO has a significant weight on the lone

(11) (a) Ziegler, T.; Rauk, A. *Theor. Chim. Acta* **1977**, *46*, 1. (b) Morokuma, K. *Acc. Chem. Res.* **1977**, *10*, 294. (c) Frenking, G. *J. Organomet. Chem.* **2001**, *635*, 9, and references therein.

(12) Bagus, P. S.; Hermann, K.; Bauschlicher, C. W. *J. Chem. Phys.* **1984**, *80*, 4378.

(13) Linares, M.; Braida, B.; Humbel, S. *Inorg. Chem.* **2007**, *46*, 11390.

(14) Mitoraj, M.; Michalak, A. *Organometallics* **2007**, *26*, 6576.

(15) (a) Pilme, J.; Silvi, B.; Alikhani, M. E. *J. Phys. Chem. A* **2003**, *107*, 4506. (b) Pilme, J.; Silvi, B.; Alikhani, M. E. *J. Phys. Chem. A* **2005**, *109*, 10028.

(16) Frisch, M. J.; Trucks, G. W.; Schlegel, H. B.; Gill, P. M. W.; Johnson, B. G.; Robb, M. A.; Cheeseman, J. R.; Keith, T.; Petersson, G. A.; Montgomery, J. A.; Raghavachari, K.; Al-Laham, M. A.; Zakrzewski, V. G.; Ortiz, J. V.; Foresman, J. B.; Cioslowski, J.; Stefanov, B. B.; Nanayakkara, A.; Challacombe, M.; Peng, C. Y.; Ayala, P. Y.; Chen, W.; Wong, M. W.; Andres, J. L.; Replogle, E. S.; Gomperts, R.; Martin, R. L.; Fox, D. J.; Binkley, J. S.; Defrees, D. J.; Baker, J.; Stewart, J. P.; Head-Gordon, M.; Gonzalez, C.; Pople, J. A. *Gaussian 94, Revision E.2* , ; Gaussian, Inc.: Pittsburgh, PA, 1995.

(17) Frisch, M. J.; Trucks, G. W.; Schlegel, H. B.; Scuseria, G. E.; Robb, M. A.; Cheeseman, J. R.; Montgomery, J. A., Jr.; Vreven, T.; Kudin, K. N.; Burant, J. C.; Millam, J. M.; Iyengar, S. S.; Tomasi, J.; Barone, V.; Mennucci, B.; Cossi, M.; Scalmani, G.; Rega, N.; Petersson, G. A.; Nakatsuji, H.; Hada, M.; Ehara, M.; Toyota, K.; Fukuda, R.; Hasegawa, J.; Ishida, M.; Nakajima, T.; Honda, Y.; Kitao, O.; Nakai, H.; Klene, M.; Li, X.; Knox, J. E.; Hratchian, H. P.; Cross, J. B.; Adamo, C.; Jaramillo, J.; Gomperts, R.; Stratmann, R. E.; Yazyev, O.; Austin, A. J.; Cammi, R.; Pomelli, C.; Ochterski, J. W.; Ayala, P. Y.; Morokuma, K.; Voth, G. A.; Salvador, P.; Dannenberg, J. J.; Zakrzewski, V. G.; Dapprich, S.; Daniels, A. D.; Strain, M. C.; Farkas, O.; Malick, D. K.; Rabuck, A. D.; Raghavachari, K.; Foresman, J. B.; Ortiz, J. V.; Cui, Q.; Baboul, A. G.; Clifford, S.; Cioslowski, J.; Stefanov, B. B.; Liu, G.; Liashenko, A.; Piskorz, P.; Komaromi, I.; Martin, R. L.; Fox, D. J.; Keith, T.; Al-Laham, M. A.; Peng, C. Y.; Nanayakkara, A.; Challacombe, M.; Gill, P. M. W.; Johnson, B. W.; Wong, W.; Gonzalez, C.; Pople, J. A. *Gaussian 03, Revision C.02*, Gaussian, Inc.: Wallingford, CT, 2004.

(18) The DZVP(Ni) basis set (Godbout, N.; Salahub, D. R.; Andzelm, J.; Wimmer, E. *Can. J. Chem.* **1992**, *70*, 560. ) was initially obtained from the Basis Set Exchange: A Community Database for Computational Sciences. Schuchardt, K.L.; Didier, B. T.; Elsethagen, T.; Sun, L.; Gurumoorthi, V.; Chase, J.; Li, J.; Windus, T. L. *J. Chem. Inf. Model.* **2007**, 10.1021/ci600510j. It is now implemented in Gaussian03.

(19) (a) te Velde, G.; Bickelhaupt, F. M.; van Gisbergen, S. J. A.; Fonseca Guerra, C.; Baerends, E. J.; Snijders, J. G.; Ziegler, T. Chemistry with ADF. *J. Comput. Chem.* **2001**, *22*, 931. (b) Fonseca Guerra, C.; Snijders, J. G.; te Velde, G.; Baerends, E. J. *Theor. Chem. Acc.* **1998**, *99*, 391. (c) *ADF2007 01*; SCM, Theoretical Chemistry, Vrije Universiteit: Amsterdam, The Netherlands, http://www.scm.com.

(20) Stefan Portmann, S.; Flükiger, P. F.; Lüthi, H. P. *Molekel 4.3*; University of Geneva and Swiss Center for Scientific Computing: Manno, Switzerland,2002, www.cscs.ch/molekel/.

(21) Bader, R. F. W. *Atoms In Molecules*; Clarendon Press: Oxford, UK, 1990.

(22) Noury, S.; Krokidis, X.; Fuster, F.; Silvi, B. *Comput. Chem.* **1999**, *23*, 597.

(23) Hochlaf, M. *J. Mol. Spectrosc.* **2001**, *210*, 284.

(24) (a) Tang, T. B.; Inokuchi, H.; Saito, S.; Yamada, C.; Hirota, E. *Chem. Phys. Lett.* **1985**, *116*, 83. (b) Klebsch, W.; Bester, M.; Yamada, K. M. T.; Winnewisser, G.; Joentgen, W.; Altenbach, H.-J.; Vogel, E. *Astron. Astrophys.* **1985**, *152*, L12. (c) McNaughton, D.; McGilvery, D.; Shanks, F. *J. Mol. Spectrosc.* **1991**, *149*, 458.

(25) Botschwina, P.; Reisenauer, H. P. *Chem. Phys. Lett.* **1991**, *183*, 217.

(26) Rienstra-Kiracofe, J. C.; Ellison, G. B.; Hoffman, B. C.; Schaefer, H. F., III *J. Phys. Chem. A* **2000**, *104*, 2273.

(27) Botschwina, P. *J. Chem. Phys.* **1989**, *90*, 4301.

(28) Moazzen-Ahmadi, N.; Zerbetto, F. *J. Chem. Phys.* **1995**, *103*, 6343.

(29) Brown, R. D.; Rice, E. H. N. *J. Am. Chem. Soc.* **1984**, *106*, 6475.

(30) Rosenblum, B.; Nethercot, A. H.; Townes, C. H. *Phys. Rev.* **1958**, *109*, 400.

(31) Muenter, J. S. *J. Mol. Spectrosc.* **1975**, *55*, 490.

(32) (a) Bader, R. F. W.; Matta, C. F. *J. Phys. Chem. A* **2004**, *108*, 8385. (b) Cortes-Guzman, F.; Bader, R. F. W. *Coord. Chem. Rev.* **2005**, *249*, 633.

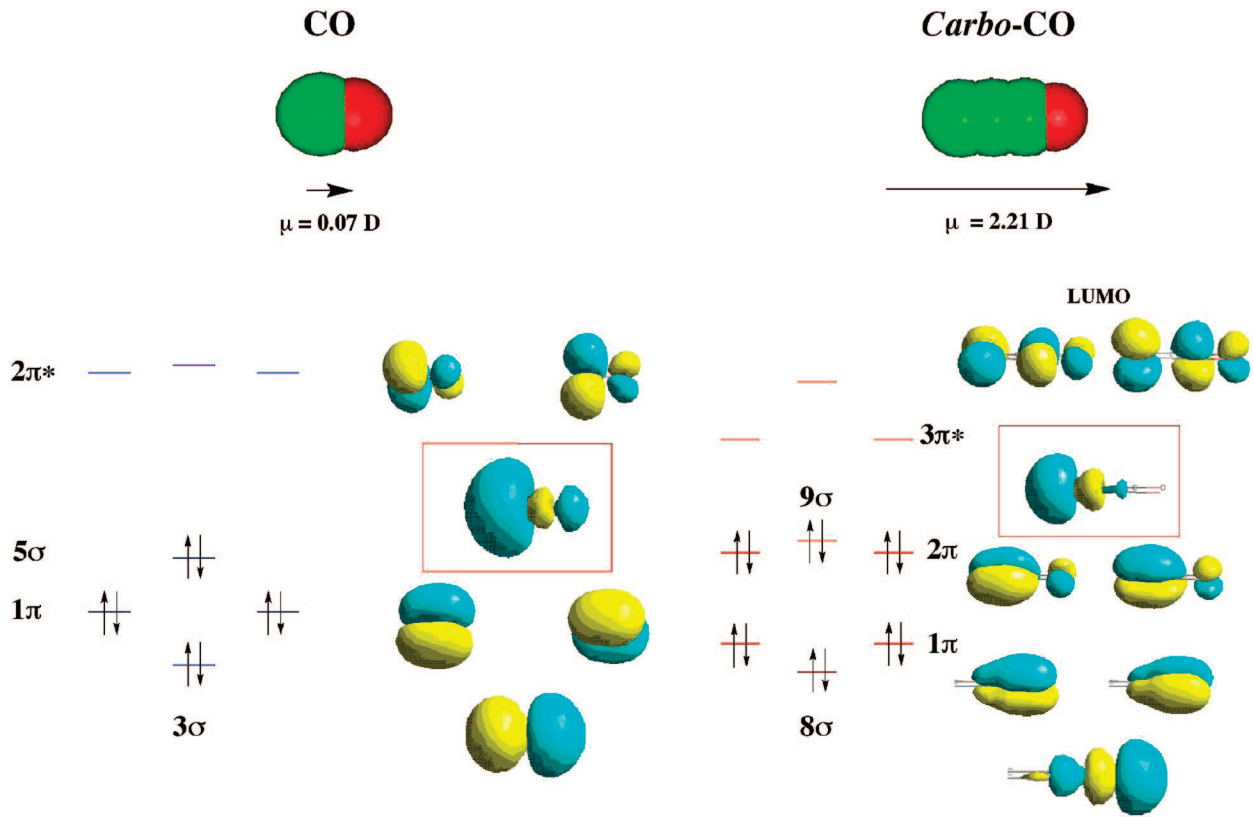


**Figure 1.** Near-frontier orbitals of CO (left) and $C_3O$ (right) at the B3LYP/6-311+G* level of calculation.

pair of the carbon end. A similar terminal coordination of the carbon terminus might therefore be anticipated for both ligands. In the case of $C_3O$, an additional $\pi$ orbital set ($2\pi$, Figure 1) localized on the **:**C═C═C moiety is of comparable amplitude on the C terminus, as it is for the parent $\pi$(C−O) orbital set ($1\pi$, Figure 1), but is closer in energy to the $\sigma$ HOMO. $C_3O$ is therefore *a priori* expected to exhibit better $\pi$-donating properties than its parent CO.

**1.c. ELF Analysis.** The ELF partition of the molecular space provides basins that correspond to classical Lewis-type electronic units such as cores, bonds, and lone pairs.[33] Their mean populations can be interpreted in terms of weighted combinations of Lewis structures.[34] A statistical analysis of the populations gives information about electron delocalization: large variance for a given basin is indicative of delocalization of its electrons, and pairwise covariance indicates the basins between which electrons are shared.[34b,35] Positive (respectively negative) covariances are indicative of correlated (respectively anticorrelated) basin populations.

The ELF analyses of CO and its *carbo*-mer have been performed (Figure 2). Although $C_3O$ exhibits two additional V(C,C) valence basins as compared to CO, the populations of the disynaptic V(C,O) and monosynaptic V(C) and V(O) basins (related to the C═O bond and the **:**C and **:**O**:** lone pairs, respectively) are very similar in both species. The scaled populations[36] and the covariance matrix ⟨cov⟩ of the ELF valence basins can be used to weight the Lewis structures required to describe the electron distribution (Figure 2). The procedure was previously disclosed in the case of carbon monoxide[34] and dinitrogen.[15b] In the case of CO and $C_3O$, the weights of the "natural" resonance forms fitting with the ELF valence basin populations and with the covariance matrix below are given in Figure 2.

$$\langle N\rangle = \begin{pmatrix} \bar{N}(\mathrm{V(C,O)}) = 3.22 \\ \bar{N}(\mathrm{V(C)}) = 2.65 \\ \bar{N}(\mathrm{V(O)}) = 4.12 \end{pmatrix}$$

$$\langle \mathrm{cov}\rangle_{\mathrm{CO}} = \begin{pmatrix} 1.41 & -0.35 & -0.84 \\ -0.35 & 0.80 & -0.31 \\ -0.84 & -0.31 & 1.38 \end{pmatrix}$$

The low weight of the all-octet shortly zwitterionic $^{-}C{\equiv}O^{+}$ form might be *a priori* surprising, as it is generally considered in the textbooks as a major contribution. This ELF picture remains however consistent with Pauling's description derived from the known physical chemistry of CO (Figure 2).[37] The $^{-}C{\equiv}O^{+}$ Lewis form was indeed invoked to account for the shortness of the C−O bond (1.12 Å) and for the orientation of the dipole moment (C→O in the physics convention, Figure 1). The sum of the ELF weights of both the $C^{-}/O^{+}$ polarized forms (38%) is indeed almost identical with Pauling's weight of the octet $^{-}C{\equiv}O^{+}$ form (40%), while the weight of the hypovalent C═O and $C^{+}{-}O^{-}$ forms are similar in both descriptions. The Lewis picture of CO derived from ELF analysis is also in agreement with the valence bond description of Maclagan et al., claiming that the apolar C═O and zwitte-

(33) (a) Becke, A. D.; Edgecombe, K. E. *J. Chem. Phys.* **1990**, *92*, 5379. (b) Silvi, B.; Savin, A. *Nature* **1994**, *371*, 683.
(34) (a) Lepetit, C.; Silvi, B.; Chauvin, R. *J. Phys. Chem. A* **2003**, *107*, 464. (b) Silvi, B. *Phys. Chem. Chem. Phys.* **2004**, *6*, 256.
(35) Savin, A.; Silvi, B.; Colonna, F. *Can. J. Chem.* **1996**, *74*, 1088.
(36) The valence populations are scaled to the actual number of electrons involved in the Lewis structures.
(37) Pauling, L. *The Nature of the Chemical Bond*, 3rd ed.; Cornell University Press: Ithaca, NY, 1960.

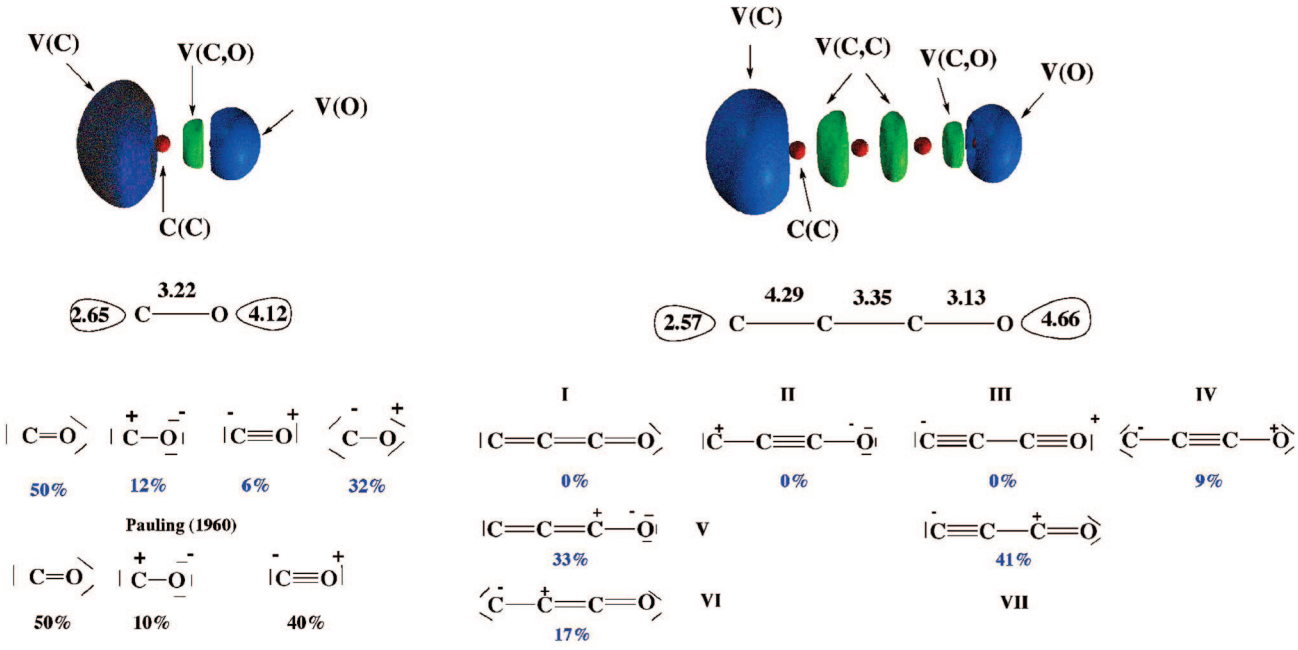


**Figure 2.** ELF analyses of CO and $C_3O$ (B3LYP/6-311+G*). (Top) Localization domains (ELF = 0.8). (Middle) Scaled populations of ELF valence basins. (Bottom) Weights of Lewis structures of CO (left) and $C_3O$ (right), derived from the scaled ELF populations.

rionic $C^-{-}O^+$ Lewis structures are prevailing.[38] Although the weight of ionic structures are expected to be both intrinsincally and indirectly overestimated (because the ELF function is here obtained from a DFT monodeterminantal evaluation of the electron density),[34b] the ELF-derived description is fully consistent with alternative analyses.

Tricarbon monoxide may be *a priori* described using the *carbo*-meric forms I−IV of the Lewis structures of the parent CO molecule (Figure 2). On the basis of a bond length analysis, Brown et al.[29] suggested a description of $C_3O$ from the three Lewis structures I−III (Figure 2). This picture is however not compatible with the ELF population vector and covariance matrix of $C_3O$ given below:

$$\langle N\rangle = \begin{pmatrix} \bar{N}(\mathrm{V(C_1)}) = 2.57 \\ \bar{N}(\mathrm{V(C_1, C_2)}) = 4.29 \\ \bar{N}(\mathrm{V(C_2, C_3)}) = 3.35 \\ \bar{N}(\mathrm{V(C_3, O)}) = 3.13 \\ \bar{N}(\mathrm{V(O)}) = 4.66 \end{pmatrix}$$

$$\langle \mathrm{cov}\rangle_{C_3O} = \begin{pmatrix} 0.78 & -0.47 & -0.12 & -0.01 & -0.04 \\ -0.47 & 1.53 & -0.65 & -0.06 & -0.08 \\ -0.12 & -0.65 & 1.42 & -0.28 & -0.14 \\ -0.01 & -0.06 & -0.28 & 1.46 & -0.91 \\ -0.04 & -0.08 & -0.14 & -0.91 & 1.43 \end{pmatrix}$$

The Lewis structure I has to be replaced by polarized structures V and VI, and structure III by structure VII. The least-squares solution of the system of linear equations linking the ELF valence scaled populations to the weights of the Lewis structures is shown in Figure 2. It is consistent with the covariance matrix elements. The large overall contribution of the Lewis structures IV, VI, and VII (67%) is in agreement with the large dipole moment of $C_3O$. Due to the low population of the C−O bond, there is no contribution of structure III:

**Table 1. Comparative Typology of Lewis Structures of CO and $C_3O$ Based on the Lewis VSEPR Character of Their Terminal Carbon Atom As Derived from ELF Analysis (B3LYP/6-311+G*)**

| class of Lewis structures | CO | $C_3O$ |
|---|---|---|
| AXE C-terminus | 68% | 74% |
| $AXE_2$ C-terminus | 32% | 26% |
| anionic C-terminus | 38% | 67% |

the **:**C−C terminus has a sizable triple-bond character in structure VII only. The analogy between CO and $C_3O$ is also illustrated by the total weights of forms involving a terminal carbon atom of given VSEPR type, which are almost identical in both species (ca. 70% AXE and 30% $AXE_2$: see Table 1). The total weight of forms involving an anionic terminal carbon $C^-$ (of either VSEPR type) is however almost twice as large as that for $C_3O$, as it could be predicted from its larger dipole moment.

**2. Coordination of $C_3O$ to Nickel. 2.a. Geometries and Bond Strengths.** The structure of the homoleptic complexes $Ni(CO)_4$ and $Ni(C_3O)_4$ have been first calculated at the B3LYP/6-31G*/DZVP(Ni) level (Table 2). Both complexes are of $T_d$ symmetry, and the calculated $Ni(CO)_4$ geometry is in excellent agreement with the one obtained by gas phase electron diffraction (Table 2).[39] However, the good performance of this hybrid all-electron 6-31G*/DZVP(Ni) basis set may be fortuitous since it results from a compromise between the performance of the Pople 6-31G* basis set (which yields a too long Ni−C bond and too short intraligand bonds) and the performance of the DZVP basis set, which shows the reverse tendency.[40]

The B3LYP/6-311+G*/SDD(Ni) level of calculation was previously used by Silvi et al. for the monocarbonyl nickel

(38) Maclagan, R. G. A. R.; Simpson, R. W. *Int. J. Quantum Chem.* **1987**, *31*, 463.

(39) (a) Hedberg, L.; Iijima, T.; Hedberg, K. *J. Chem. Phys.* **1979**, *70*, 3224. (b) Braga, D.; Grepioni, F.; Orpen, A. G. *Organometallics* **1993**, *12*, 1481.

(40) (a) Godbout, N.; Salahub, D. R.; Andzelm, J.; Wimmer, E. *Can. J. Chem.* **1992**, *70*, 560. (b) Sosa, C.; Andzelm, J.; Elkin, B. C.; Wimmer, E.; Dobbs, K. D.; Dixon, D. A. *J. Phys. Chem.* **1992**, *96*, 6630.

(41) (a) Day, J. P.; Basolo, F.; Pearson, R. G. *J. Am. Chem. Soc.* **1968**, *90*, 6927. (b) Stevens, A. E.; Feigerle, C. S.; Lineberger, W. C. *J. Am. Chem. Soc.* **1982**, *104*, 5026.

(42) Daprich, S.; Pidun, U.; Ehlers, A. W.; Frenking, G. *Chem. Phys. Lett.* **1995**, *242*, 521.

**Table 2. *Carbo*-meric Comparison of Bond Lengths (in Å) and First Dissociation Energies $D_e$ (in kcal mol$^{-1}$) of Nickel Carbonyl Complexes at Various Levels of Calculation**

| complex | basis set | Ni−$C_1$ | $C_1$−$C_2$ | $C_2$−$C_3$ | $C_3$−O | $D_e$[c] | $D_e$(corr)[d] |
|---|---|---|---|---|---|---|---|
| $Ni(CO)_4$ | exptl[a] | 1.838 | | | 1.141 | 22−27[b] | |
| | 6-31G*/LANL2DZ(Ni) | 1.851 | | | 1.145 | 18.4 | 16.6 |
| | 6-31G*/DZVP(Ni) | 1.836 | | | 1.146 | 23.0 | 21.0 |
| | 6-311+G* | 1.845 | | | 1.137 | 20.2 | 18.3 |
| | 6-311+G*/SDD(Ni) | 1.841 | | | 1.137 | 20.2 | 18.2 |
| $Ni(C_3O)_4$ | 6-31G*/DZVP(Ni) | 1.801 | 1.274 | 1.291 | 1.168 | 29.9 | |
| | 6-311+G* | 1.813 | 1.270 | 1.286 | 1.158 | 29.9 | 27.8 |
| | 6-311+G*/SDD(Ni) | 1.808 | 1.269 | 1.286 | 1.158 | 29.3 | 27.4 |
| $Ni(C_3O)(CO)_3$ | 6-31G*/DZVP(Ni) | 1.802 | 1.274 | 1.292 | 1.167 | 37.0 | 35.3 |
| | 6-311+G* | 1.813 | 1.269 | 1.288 | 1.157 | 35.7 | 33.4 |
| | 6-311+G*/SDD(Ni) | 1.805 | 1.269 | 1.287 | 1.157 | 35.9 | 33.5 |
| free CO | exptl[e] | | | | 1.128 | | |
| | 6-311+G* | | | | 1.128 | | |
| free $C_3O$ | exptl[f] | | 1.254 | 1.306 | 1.153 | | |
| | 6-311+G* | | 1.270 | 1.295 | 1.150 | | |

[a] Structural data from ref 39. [b] From ref 41. [c] Crude first dissociation energy of the largest ligand. [d] First dissociation energy of the largest ligand including vibrational zero-point energy corrections. [e] From ref 7b. [f] From ref 3.

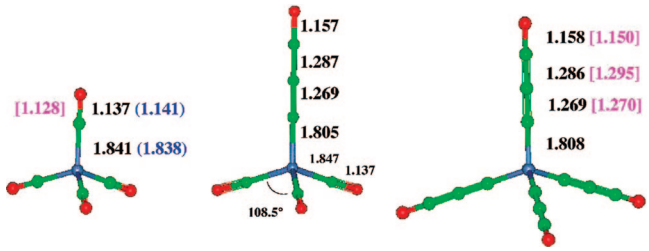


**Figure 3.** Comparison of calculated structures of $Ni(CO)_4$ ($T_d$), $Ni(C_3O)(CO)_3$ ($C_{3v}$), and $Ni(C_3O)_4$ ($T_d$) complexes (B3LYP/6-311+G*/SDD(Ni)). Bond lengths are given in Å. Experimental bond distances are in parentheses and calculated bond lengths of the free ligands are in square brackets.

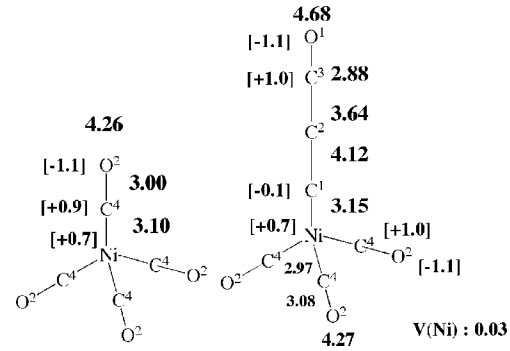


**Figure 4.** Average populations of ELF basins in $Ni(CO)_4$ and $Ni(C_3O)(CO)_3$. AIM charges in square brackets. BLYP/6-311G* values given here are comparable to the B3LYP/6-311G* ones (Table 3).

complex,[15] as it allows for a reliable description of the two lowest electronic configurations of nickel atom. It was therefore selected for this work. The $Ni(CO)_4$ geometry calculated at this level is indeed in excellent agreement with the experimental one (Table 2), while calculations performed with the all-electrons 6-311+G** basis set or the LANL2DZ pseudopotential are less satisfactory (Table 2).

The structure of the heteroleptic complex $Ni(C_3O)(CO)_3$ of $C_{3v}$ symmetry has also been calculated. The geometry of the $C_3O$ ligand is similar in $Ni(C_3O)_4$ and in $Ni(C_3O)(CO)_3$ (Table 2). In particular, the $\eta^1$-C-coordination of $C_3O$ remains the most favorable. Among the three possible isomers of $Ni(C_3O)(CO)_3$ exhibiting a dihapto coordination of $C_3O$, only $Ni(\eta^2$-$C{\equiv}CCO)(CO)_3$ is stable but is 27.9 kcal/mol higher in energy than $Ni(CO)_3(\eta^1$-$C_3O)$ at the B3LYP/6-311+G*/SDD(Ni) level. The O-coordination of $C_3O$ is unstable. $C_3O$ and CO exhibit therefore the same terminal $\eta^1$-C-coordination mode.

The Ni−C bond length in $Ni(C_3O)_4$ and in $Ni(C_3O)(CO)_3$ is shorter than in $Ni(CO)_4$ (Figure 3). This suggests that $C_3O$ is more strongly bound to nickel than its parent CO. In contrast, the C−O bond length in $Ni(C_3O)_4$ is longer than in $Ni(CO)_4$. The variation of the C−O bond length upon nickel coordination is however the same, about 0.008 Å (Figure 3), suggesting a comparable $\pi$-back-bonding in both case. The terminal C−C bond length of $C_3O$ is little affected by the bonding to nickel. $\pi$-Donation is thus expected to be weak.

The Ni−C bond strengths were also estimated from the first dissociation energies. Crude dissociation energies without zero-point and basis set superposition error (BSSE) corrections are given in Table 2. The B3LYP/6-31G*/DZVP(Ni) level of calculation yields again a good agreement with the reported experimental dissociation energy of $Ni(CO)_4$[41] and with CCSD(T)//MP2 calculations.[42] The 6-311+G*/SDD(Ni) and 6-311+G* basis sets remain more satisfactory than the 6-31G*/LANL2DZ(Ni) basis set. At the three different levels used here however, the calculated first dissociation energy of $C_3O$ from $Ni(C_3O)_4$ and from $Ni(C_3O)(CO)_3$ is larger than the one of CO from $Ni(CO)_4$ by ca. 10 and 15 kcal mol$^{-1}$, respectively (Table 2). This indicates that $C_3O$ is definitely more strongly bound to nickel than its parent CO.

**2.b. Comparaison of Donor−Acceptor Properties of CO and its *Carbo*-mer.** The donor−acceptor properties of CO and its *carbo*-mer are hereafter compared with respect to the same $Ni(CO)_3$ fragment. By comparison to the homoleptic complex $Ni(C_3O)_4$ (that would afford less comparative analyses), the $C_{3v}$ symmetry of the selected $Ni(C_3O)(CO)_3$ complex is expected to allow for an easier separation of $\sigma$ and $\pi$ interactions.

The results of ELF and AIM analyses for $Ni(CO)_4$ and $Ni(C_3O)(CO)_3$ are detailed in Figure 4 and Figure 5. The average populations of selected ELF basins are given in Table 3 at various calculation levels. Within the errors bars, these populations are barely sensitive to the DFT level. The less reliable HF level yields a population of the Ni−C bond lower than that obtained at the DFT level. The reverse holds for the C−O bond. This effect is a consequence of the electron correlation: the monosynaptic basin population calculated with correlated wave functions are usually larger than the HF ones, whereas disynaptic basins are less populated. In the present system, the V(Ni,C)

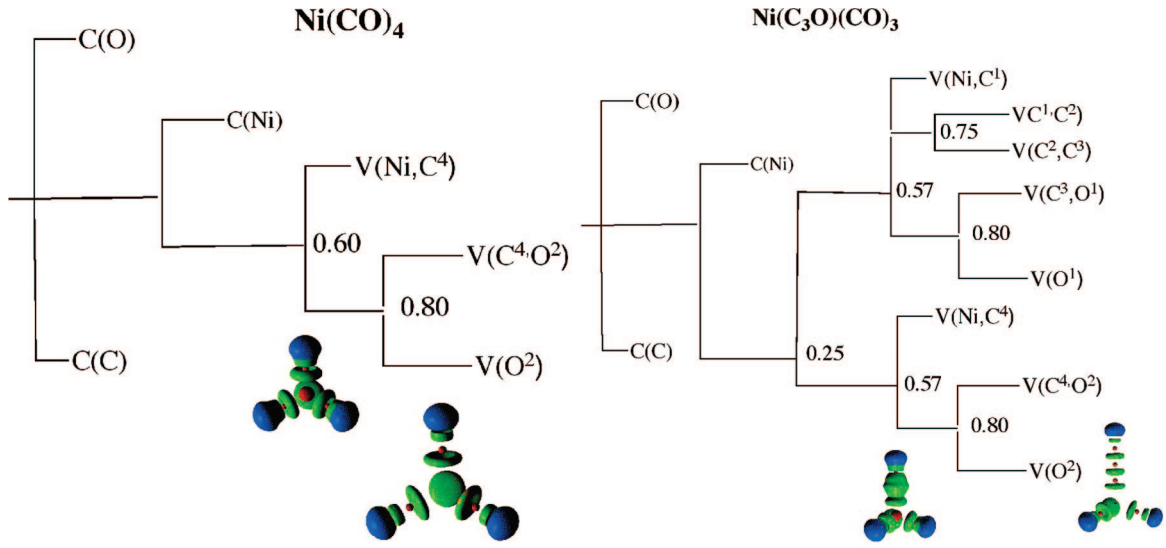


**Figure 5.** Localization reduction diagram of $Ni(CO)_4$ (left) and $Ni(C_3O)(CO)_3$ (right).

**Table 3. Average Populations of Selected ELF Basins in $Ni(C_3O)(CO)_3$ and $Ni(CO)_4$ Calculated at Various Levels with the 6-311G* Basis Set[a]**

| complex/calc level | V(Ni,$C^1$) | V($C^1$,$C^2$) | V($C^2$,$C^3$) | V($C^3$,$O^1$) | V($O^1$) | V(Ni,$C^4$) | V($C^4$,$O^2$) | V($O^2$) | V(Ni)[c] | C(Ni) | $\delta q$[b] |
|---|---|---|---|---|---|---|---|---|---|---|---|
| $Ni(C_3O)(CO)_3$ | | | | | | | | | | | |
| B3LYP | 3.12 | 4.17 | 3.53 | 2.94 | 4.68 | 2.99 | 3.04 | 4.26 | 0.05 | 25.65 | 2.30 |
| BLYP | 3.15 | 4.12 | 3.64 | 2.88 | 4.68 | 3.08 | 2.97 | 4.27 | 0.03 | 25.54 | 2,43 |
| PBE | 3.15 | 4.11 | 3.19 | 2.90 | 4.66 | 3.08 | 2.99 | 4.26 | 0.05 | 25.49 | 2.46 |
| HF | 2.85 | 4.41 | 3.24 | 3.01 | 4.72 | 2.72 | 3.22 | 4.23 | 0.09 | 25.48 | 2.43 |
| $Ni(CO)_4$ | | | | | | | | | | | |
| B3LYP | | | | | | 3.02 | 3.06 | 4.25 | | 25.89 | 2.11 |
| BLYP | | | | | | 3.10 | 3.00 | 4.26 | | 25.74 | 2.26 |
| PBE | | | | | | 3.11 | 3.00 | 4.26 | | 25.68 | 2.32 |
| HF | | | | | | 2.74 | 3.23 | 4.23 | | 26.43 | 1.57 |

[a] Geometries calculated at the B3LYP/6-311+G*/SDD(Ni) level. Atom numbering in $C_{3v}$ symmetry: Ni($C^1$=$C^2$=$C^3$=$O^1$)($C^4$=$O^2$)$_3$ and Ni($C^4$=$O^2$)$_4$. [b] Net electron density transfer toward ligands $\delta q = 28 - C(Ni) - V(Ni)$. See ref 15a. [c] The presence of monosynaptic valence basins V(Ni) of very low population may be ascribed to the use of diffuse basis functions that may indirectly induce oscillations in the regions of low ELF values.

basin corresponds to the V(C) basin of the uncomplexed moieties. This result is consistent with the calculations of Matito et al.[43]

The ELF populations of the Ni−C and C−O bonds are quite similar in both complexes and are indicative of a sizable double-bond character of the Ni−C bond, which is slightly larger in $Ni(C_3O)(CO)_3$. This is in line with the stronger Ni−$C_3O$ bond indicated by the dissociation energy values (see section 2a).

The $C_2$−$C_3$ bond is slightly shortened upon coordination of $C_3O$ to nickel (Table 2 and Figure 3), while the ELF population of the disynaptic basin V($C^2$,$C^3$) increases upon attachment of $C_3O$ to the $Ni(CO)_3$ moiety (Figure 2 and Table 3). This may be related to the $\pi$-back-donation from the d orbitals of nickel to the $3\pi^*$ LUMO of $C_3O$ (Figure 1). Similar geometrical trends were found upon coordination of CNCN to chromium in the $Cr(CO)_5$(CNCN) complex.[7b] The $3\pi^*$ LUMO of the isoelectronic $C_3O$ and CNCN ligands is indeed similar and exhibits an antibonding character in the $C_1$−$C_2$ and C−NCN bonds and a bonding character in the $C_2$−$C_3$ and CN−CN bonds.

In the localization reduction diagram (Figure 5),[35,44] it is noticeable that, in contrast to what was observed in *carbo*-heterocycles, the oxygen atom of $C_3O$ preserves its valence structure at a higher ELF value than the inserted $C_2$ unit does.[45]

The net electron transfer from nickel toward ligands may be estimated by $\delta q = Z - C(Ni) - V(Ni)$ and is reported in Table 3.[15a] The large positive $\delta q$ values are little sensitive to the calculation level (Table 3). They are larger in the presence of a $C_3O$ ligand and are indicative of an average electron transfer from nickel to each ligand larger than 0.5 e.

Within the DCD scheme, the $\sigma$-donation (respectively $\pi$-donation) is defined as a ligand-to-metal charge transfer (so-called LMCT) that involves the canonical orbitals of $\sigma$ symmetry (respectively $\pi$ symmetry). The back-donation is the contribution of the $\pi$ canonical orbitals in the opposite MLCT direction. As the ELF and AIM partitions allow to distinguish between the metal and ligand moieties, it is possible to quantify the donation and back-donation from the contributions of the orbitals of the desired symmetry to the basins of one of the moieties.[15a] The results are detailed below.

**2.b.1. $Ni(CO)_4$.** The near-frontier occupied molecular orbitals of $Ni(CO)_4$ of $T_d$ symmetry are displayed in Figure 6a. From the fragment analysis performed with the ADF code (four equivalent CO fragments on one hand and one nickel atom on the other hand), it is clear that the DCD description of the metal−CO bonding is a simplified qualitative summary of the true MO diagram.[46] The near-frontier occupied orbitals result from the primary LMCT and MLCT interactions mentioned above, but also from the interaction with other MOs of the fragments that possess the same symmetry and are close in energy. For example, the #40−42 or 9T2 MO set undergoes a

(43) Matito, E.; Silvi, B.; Duran, M.; Sola, M. *J. Chem. Phys.* **2006**, *125*, 024301.
(44) Calatayud, M.; Andres, J.; Beltran, A.; Silvi, B. *Theor. Chem. Acc.* **2001**, *105*, 299.
(45) Lepetit, C.; Peyrou, V.; Chauvin, R. *Phys. Chem. Chem. Phys.* **2004**, *6*, 303.
(46) Frenking, G.; Fröhlich, N. *Chem. Rev.* **2000**, *100*, 717.

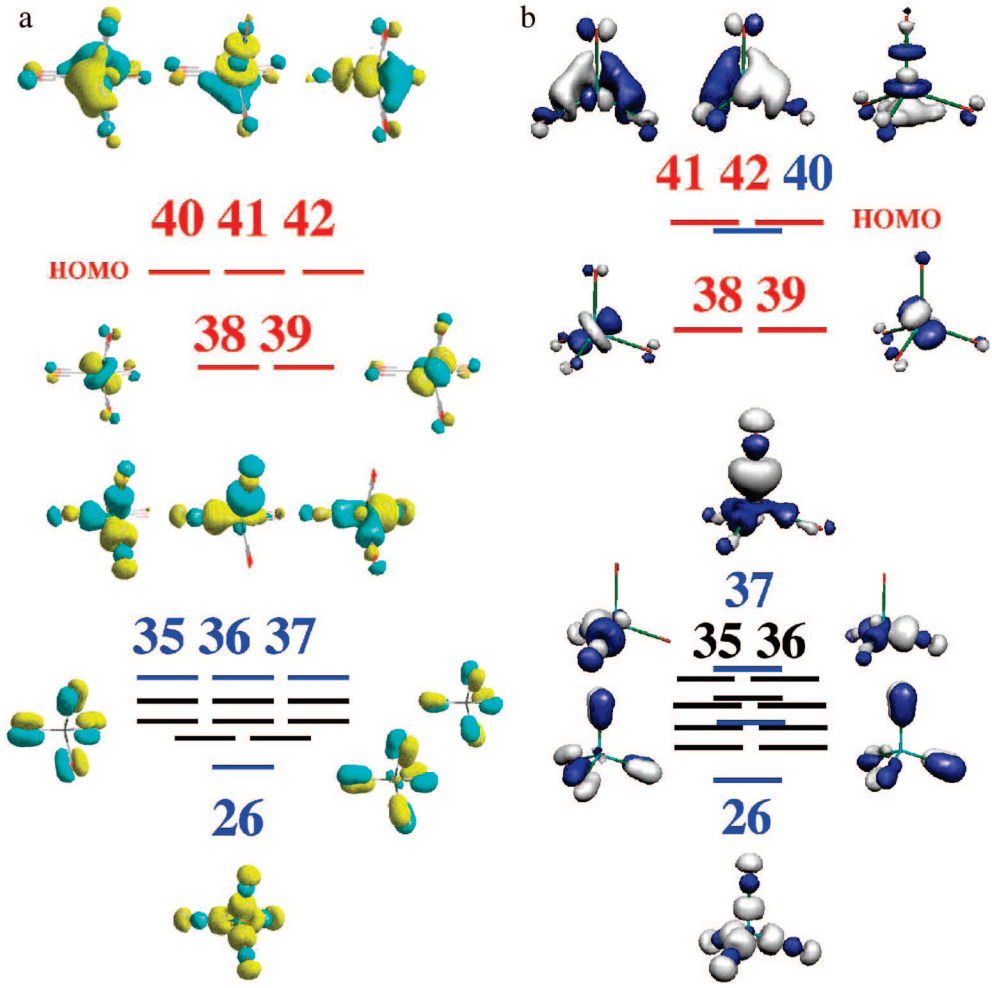


**Figure 6.** (a) Occupied near-frontier MOs of $Ni(CO)_4$ of $T_d$ symmetry (B3LYP/6-311G*). (b) Occupied near-frontier MOs of $Ni(CO)_4$ of $C_{3v}$ symmetry (B3LYP/6-311G*). MOs involved in $\sigma$-donation are highligted in blue, while the those involved in $\pi$-back-donation are highlighted in red.

residual symmetry-allowed $\sigma/\pi$ mixing (Figure 6a) that prevents a fair estimation of the donor−acceptor properties of the CO ligand to nickel (see Supporting Information).

Infinitesimal lowering of the symmetry of $Ni(CO)_4$ to $C_{3v}$ allows for the clear-cut separation of $\sigma$ and $\pi$ interactions and for a more direct comparison with the $Ni(C_3O)(CO)_3$ complex. The near-frontier occupied MOs of $Ni(CO)(CO)_3$, where one Ni−C bond was elongated by 0.001 Å, are displayed in Figure 6b.

The ADF fragment analysis based on a $Ni(CO)_3$ fragment and one CO fragment pointing in the symmetry axis direction allows to easily distinguish between three sets of MOs (Table S2).

• Two sets of degenerate MOs, #38−39 and #41−42 (11E1 and 12E1), are related to $\pi$-back-donation ($\pi$b), as they result from the interaction of occupied MOs of the $Ni(CO)_3$ fragment with the empty $2\pi^*$ MO of the CO fragment.

• Four MOs, i.e., #26, 31, 37, and 40 (14−17 A1), are related to $\sigma$-donation ($\sigma$d), because of a sizable contribution of the $5\sigma$ of CO and almost no mixing with the $4\sigma$ or $3\sigma$ MOs of CO.

• Eight MOs, #27−30, #32−33, and #35−36 (7−10E1), exhibit a contribution the $1\pi$ MO of the CO fragment and can thus be related to "$\pi$-donation" ($\pi$d), although there is no contribution of any empty MO of the $Ni(CO)_3$ fragment (an offering is not always accepted but remains an offering).

**Table 4. Donor−Acceptor Contributions of the CO Ligand toward the $Ni(CO)_3$ Fragment in the $Ni(CO)(CO)_3$ Complex of $C_{3v}$ Symmetry, Obtained from AIM and ELF Analyses Performed at Various Calculation Levels 6-311G* Basis Set and B3LYP/6-311+G*/SDD(Ni) Level of Calculation for Geometries**

| | ELF | | | AIM | | |
|---|---|---|---|---|---|---|
| calculation method | $\sigma$d | $\pi$d | $\pi$b | $\pi$b | $\delta q'^{a}$ | $\delta q/4^{b}$ |
| B3LYP | 0.10 | 0.06 | 0.62 | 0.48 | 0.55 | 0.53 |
| BLYP | 0.07 | 0.05 | 0.69 | 0.52 | 0.57 | 0.57 |
| PBE | 0.09 | 0.03 | 0.69 | 0.52 | 0.57 | 0.58 |
| HF | 0.10 | 0.07 | 0.48 | 0.36 | 0.31 | 0.39 |

[a] Net electron transfer from nickel toward each CO ligand, $\delta q' = \pi b - (\sigma d + \pi d)$. [b] $\delta q$ values ($\delta q = 28 - C(Ni)$) from Table 3.

In the AIM scheme, only the $\pi$-back-donation may be calculated from the contribution of the 11−12E1 sets to the carbon and oxygen atomic basins. Thus, at the B3LYP/6-311G* level of calculation, $\pi b_{AIM} = 0.48$ e$^-$ (Table 4).

In the ELF scheme, the $\sigma$ and $\pi$ contributions arising from the above three sets of orbitals to the core basins C(O) and C(C) and to the valence basins V(C,Ni), V(C,O), and V(O) of one of the CO ligands are considered (Table S3). The $\pi$-back-donation, $\sigma$-donation, and $\pi$-donation in $Ni(CO)_4$ can thus be estimated at the B3LYP/6-311G* level of calculation as shown:

$$\sigma d_{ELF} = 2 - (0.47 + 0.01 + 1.20 + 0.22) = 0.10\ e^-$$

$$\pi d_{ELF} = 4 - (2.47 + 1.45 + 0.02) = 0.06\ e^-$$

$$\pi b_{ELF} = (0.25 + 0.37) = 0.62\ e^-$$

The results are little sensitive to the calculation level (Table 4) and definitely show that the major effect is a $\pi$-acceptance of the CO ligand (ca. 5 times the $\sigma$d and $\pi$d effects).

The net electron transfer from nickel toward each CO ligand via the selected fragment MOs, denoted as $\delta q'$ and calculated from the relative contributions of Table 4, is in very good agreement with the global transfer estimated previously from the C(Ni) population (Table 3). The coordination of one CO ligand is accompanied by a net electron transfer of about 0.57 e from the nickel center to each CO ligand. The total transfer of about 2.30 e is larger than the 1.02 e estimated from the ELF analysis in nickel monocarbonyl NiCO (the Ni−CO transfer is of course not additive).[15a] In both complexes, these results are consistent with a large contribution of the ionic $(CO)_3Ni^+(CO)^-$ Lewis form. The AIM charge of +0.6 of Ni in the $Ni(CO)_4$ complex is also consistent with this suggestion.

CO appears therefore to be essentially a $\pi$-accepting ligand. This large $\pi$-acceptance ability is consistent with other claims in the literature. Most of the studies devoted to the analysis of the transition metal−CO interactions, mainly based on energy partition techniques, indeed concluded that $\pi$-back-donation is more important than $\sigma$-donation.[47] It was indeed shown on the basis of energy decomposition analysis that the stabilization that comes from $\pi$-back-donation contributes 54% to the total orbital interactions, while 46% comes from $\sigma$-donation.[47b] AIM analyses of either experimental or theoretical gas phase electron densities are also consistent with a significant $\pi$-back-donation.[32,48] Only studies based on CDA/NBO analyses concluded a $\pi$-back-donation smaller than the $\sigma$-donation.[49] More recent reports have however underlined that this method may be misleading because it intrinsically overestimates the extent of $\sigma$-donation.[50] This could be related to previous observations that the ELF mesomeric description of a molecule generally involves more ionic Lewis structures than the corresponding NBO/NRT picture. The origin of the discrepancy might be ascribed to the nature of the NRT mesomeric structures, which are of the Coulson−Fisher type. As they are polarized, they implicitly account for ionic components. The $\pi$-back-bonding is indeed formally represented by the no-bond $Ni^+(CO)^-$ resonance form suggested by ELF analysis,[15] while the $\sigma$-donation is not represented by a ionic form but by a classical semipolar $Ni^-$–$(CO)^+$ resonance form.

**2.b.2. $Ni(C_3O)(CO)_3$.** The donor−acceptor properties of $C_3O$ toward the same $Ni(CO)_3$ fragment may be evaluated following a similar procedure for the $Ni(C_3O)(CO)_3$ complex. From the MO interaction diagram (Figure 7) and the ADF fragment analysis into one $Ni(CO)_3$ and one $C_3O$ fragments (Table S4), the MOs are now classified into three groups.

• The set of degenerate MOs #46−47 (13E1) is related to $\pi$-back-donation, because they exhibit a sizable contribution of occupied MOs of the $Ni(CO)_3$ fragment and of the $3\pi$ and $4\pi$ empty MOs of the $C_3O$ fragment (Table S4).

• Three MOs are related to $\sigma$-donation: #48 (HOMO), 41 and 30 (21−20A1 and 18A1). From the ADF fragment analysis they indeed show a sizable contribution of the $9\sigma$ MOs of $C_3O$ and no mixing with the $8\sigma$ or $7\sigma$ MOs of $C_3O$ (Table S4).

• Two sets of degenerate MOs might be related to "$\pi$-donation"—#42−43 and #44−45 (11−12E1)—although they do not involve any acceptance of empty MOs of the $Ni(CO)_3$ fragment (Table S4).

Following the same procedure as above, in the AIM scheme, the $\pi$-back-donation is therefore estimated from the contribution of the 13E1 $\pi$ orbitals to atomic basins of the ligand. The $\pi b_{AIM}$ values of $Ni(C_3O)(CO)_3$ (Table 5) are larger by 0.2−0.3 e than those of $Ni(CO)_4$ (Table 4).

The $\sigma/\pi$-donation/back-donation components derived from ELF analysis and given in Table 5 are now more sensitive to the level of calculation. DFT/GGA calculations suggest that $C_3O$ exhibits slightly stronger $\sigma$-donating and $\pi$-accepting properties than its CO parent (Table 5), whereas HF and hybrid DFT calculations also suggest a sizable $\pi$-donation ability of $C_3O$. The latter is however questionable.

(i) The terminal $C_1-C_2$ bond length of $C_3O$ is little affected by coordination to nickel, and beyond putative DFT cancelation of errors, this might naturally reflect the weakness of $\pi$-donation.

(ii) No evidence of any interaction between the $2\pi$ MO of $C_3O$ with an empty MO of the $Ni(CO)_3$ fragment could be extracted from the ADF fragment analysis (Table S4).

In contrast to $Ni(CO)_4$, the occupied $2\pi$ MO of $C_3O$ contributes to the degenerate #46−47 or 13E1 MO set assigned to $\pi$-back-donation (Figure 7). At the HF and B3LYP levels of calculation, this contribution is sizable, namely, twice the one obtained at the pure DFT level (Table S4). This result therefore rules out the possibility of distinguishing between $\pi$-donation and $\pi$-back-donation. The DFT/GGA calculations (BLYP and PBE) are therefore reliable, as they do not suffer from this drawback. PBE calculations have been selected for the final discussion hereafter.

From the ELF and AIM analysis, the stronger Ni−$C_3O$ bond as compared to the Ni−CO bond (Table 2) may be mostly related to the stronger $\pi$-acceptance ability of $C_3O$ as compared to its CO parent (Table 6). Both ligands exert a negligible $\sigma$-donation. This is in line with previous reports concluding that nickel−CO bonding involves $\sigma$-repulsion and $\pi$-back-donation.[46,51]

The coordination of $C_3O$ results in a net electron transfer of about 0.70 e from Ni to $C_3O$ (Table 5). It is larger by about 0.2 e than the electron transfer from Ni to the parent CO in $Ni(CO)_4$ (Table 4) and is roughly equivalent to the variation of the sole $\pi$-back-donation. This is also consistent with the same 0.2 e difference between the $\delta$q values in $Ni(C_3O)(CO)_3$ and $Ni(CO)_4$ complexes (Table 3). A sizable contribution of the ionic no-bond $(CO)_3Ni^+(C_3O)^-$ Lewis structure has thus to be invoked.

## Conclusion

The coordinating properties to nickel of CO and *carbo*-CO have been compared. From the present calculations, the Ni−$C_3O$ bond is predicted to be stronger than the corresponding Ni−CO bond. Coordination chemistry appears as an alternative way to stabilize this heterocumulene, mainly studied in argon matrixes and interstellar clouds hitherto.

ELF and AIM analysis have been used to estimate the donation and back-donation contributions to the net charge transfer occurring in three nickel complexes of CO and $C_3O$. The $\sigma$-donating and $\pi$-accepting properties of $C_3O$ toward $Ni(CO)_3$ are slightly stronger than for its CO parent. In both cases, however, $\pi$-back-donation is the prevailing electron transfer mode.

(47) (a) Frenking, G.; Wichmann, K.; Fröhlich, N.; Loschen, C.; Lein, M.; Frunzke, J.; Rayon, V. M. *Coord. Chem. Rev.* **2003**, *238* (239), 55. (b) Doerr, M.; Frenking, G. *Z. Anorg. Allg. Chem.* **2002**, *628*, 843.

(48) (a) Macchi, P.; Sironi, A. *Coord. Chem. Rev.* **2003**, *238* (239), 383. (b) Farrugia, L. J.; Evans, C. *J. Phys. Chem. A* **2005**, *109*, 8834.

(49) (a) Ehlers, A. W.; Dapprich, S.; Vyboishchikov, S. F.; Frenking, G. *Organometallics* **1996**, *15*, 105. (b) Petz, W.; Weller, F.; Uddin, J.; Frenking, G. *Organometallics* **1999**, *18*, 619.

(50) Garcia Hernandez, M.; Beste, A.; Frenking, G.; Illas, F. *Chem. Phys. Lett.* **2000**, *320*, 222.

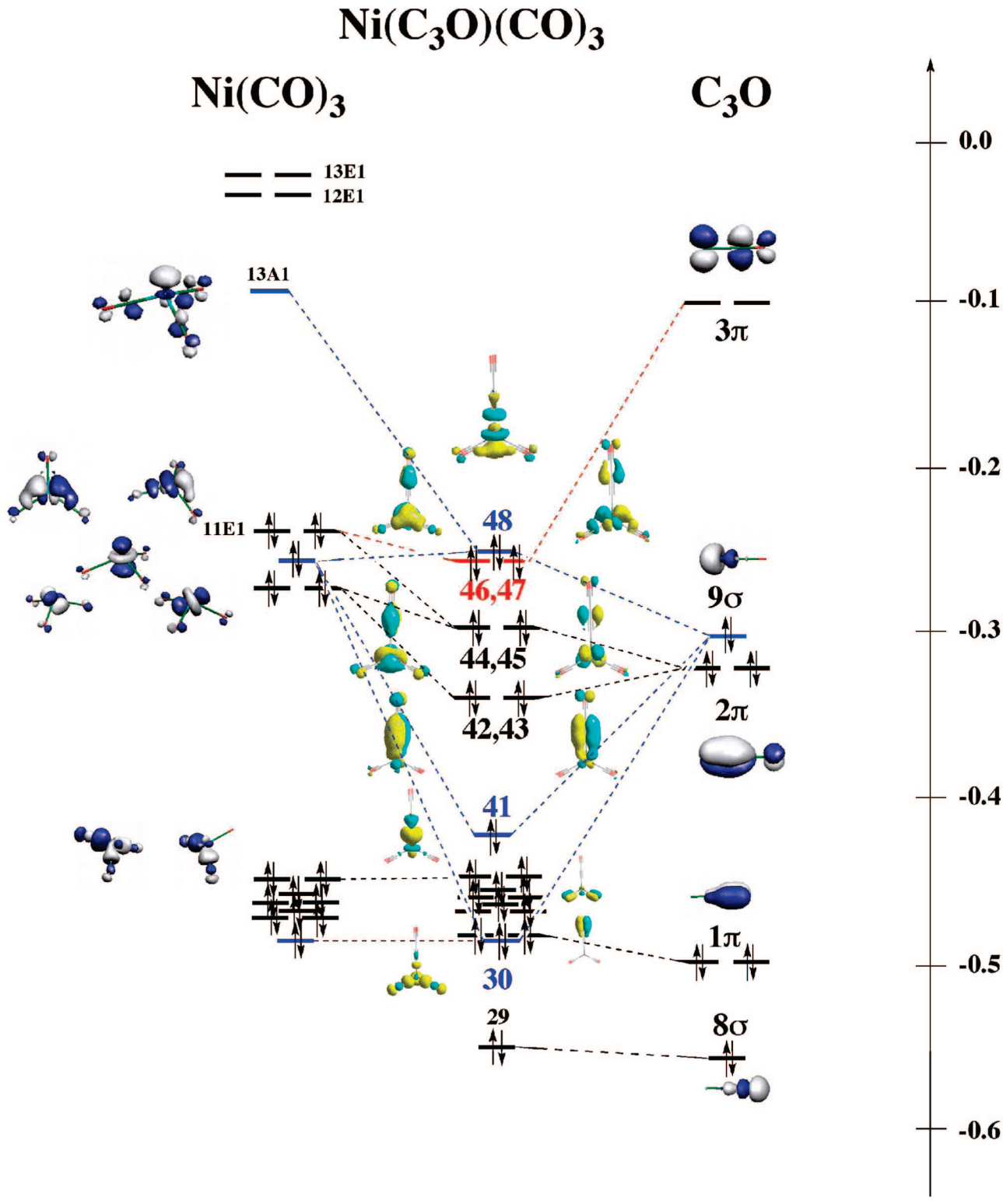


**Figure 7.** Molecular orbital (interaction) diagram of $Ni(C_3O)(CO)_3$ of $C_{3v}$ symmetry (B3LYP/6-311G*). MOs involved in $\sigma$-donation are highligted in blue, while the ones involved in $\pi$-back-donation are highlighted in red. Energy scale in hartrees.

An added value for this method, in the case of $Ni(CO)_4$, is its low sensitivity to the level of calculation, although the orbital overlap between the interacting fragments was expected to depend on it.[52] In contrast to HF calculations that overestimate the HOMO−LUMO gap, DFT tends to shrink this gap and is therefore expected to overestimate the electron transfer. Hybrid functionals may therefore be a good compromise. However, in the $Ni(C_3O)(CO)_3$ case, pure DFT was found to be the only reliable calculation level.

More generally, provided that the molecular orbitals involved in the various (back-)donation modes are easily identified and well separated by choosing a suitable symmetry, the present method based on ELF and AIM analyses allows for the clear-

(51) Nyberg, N.; Föhlisch, A.; Triguero, L.; Bassan, A.; Nilsson, A.; Pettersson, L. G. M. *J. Mol. Struct.: THEOCHEM* **2006**, *762*, 123.
(52) Stowasser, R.; Hoffmann, R. *J. Am. Chem. Soc.* **1999**, *121*, 3414.

**Table 5. Donor−Acceptor Contributions of the $C_3O$ Ligand toward the $Ni(CO)_3$ Fragment in the $Ni(C_3O)(CO)_3$ Complex, Obtained from AIM and ELF Analyses Performed at Various Calculation Levels (6-311G* Basis Set and B3LYP/6-311+G*/SDD(Ni) Level of Calculation for Geometries; See Table S5 for Details)**

| | ELF | | | AIM | |
|---|---|---|---|---|---|
| calculation method | $\sigma$d | $\pi$d | $\pi$b | $\pi$b | $\delta q'^{a}$ |
| B3LYP | 0.13 | 0.22 | 0.92 | 0.56 | 0.57 |
| BLYP | 0.14 | 0.01 | 0.89 | 0.74 | 0.74 |
| PBE | 0.16 | 0.00 | 0.88 | 0.74 | 0.72 |
| HF | 0.11 | 0.36 | 0.94 | 0.84 | 0.47 |

[a] Net electron density transfer from nickel toward the $C_3O$ ligand: $\delta q' = \pi b - (\sigma d + \pi d)$.

**Table 6. Comparison of the Donor−Acceptor Properties of CO and $C_3O$ toward $Ni(CO)_3$ (PBE/6-311G*)**

| complex | method | $\sigma$d | $\pi$d | $\pi$b |
|---|---|---|---|---|
| $Ni(CO)_4$ | AIM | | | 0.52 |
| | ELF | 0.09 | 0.03 | 0.69 |
| $Ni(C_3O)(CO)_3$ | AIM | | | 0.74 |
| | ELF | 0.16 | 0.00 | 0.88 |

cut quantification of electron transfers in transition metal complexes. It calls for further validation, but it stands as a promising candidate for refining or even qualifying the conclusions of the DCD approximate description.

**Acknowledgment.** The authors would like to thank CALMIP (Calcul intensif en Midi-Pyrénées, Toulouse, France), IDRIS (Institut du Développement et des Ressources en Informatique Scientifique, Orsay, France), and CINES (Centre Informatique de l'Enseignement Supérieur, Montpellier, France) for computing facilities and the Ministère de l'Education Nationale de la Recherche et de la Technologie for ACI financial support. The authors would also like to thank Professor Henry Chermette for his help in ADF fragment analyses.

**Supporting Information Available:** ELF/DCD analysis of $Ni(CO)_4$ of $T_d$ symmetry. Tables S1−S5: Cartesian coordinates, total energies, and ZPE-corrected values in atomic units (B3LYP/6-311+G*/SDD(Ni) level of calculation) for the $Ni(C_3O)(CO)_3$ complex of $C_{3v}$ symmetry and $Ni(C_3O)_4$ complex of $T_d$ symmetry. This material is available free of charge via the Internet at http://pubs.acs.org.

OM800578C